JOURNAL OF WATER AND LAND DEVELOPMENT
e-ISSN 2083-4535
Polish Academy of Sciences (PAN) Institute of Technology and Life Sciences – National Research Institute (ITP – PIB)

JOURNAL OF WATER AND LAND DEVELOPMENT
DOI: 10.24425/jwld.2021.139943
2022, No. 52 (I–III): 53–59

Experimental and numerical investigation of scour downstream contracted spillways

Tarek H. Nasralla ✉

Benha University, Benha Faculty of Engineering, Civil Engineering Department, 13512, Benha, Qalubiya, Egypt

RECEIVED 11.12.2020 REVIEWED 28.01.2021 ACCEPTED 28.06.2021

Abstract: A study of scour downstream of free hydraulic jump in stilling basin of stepped spillways was carried out. This paper employed an experimental study to investigate the stepped spillway with the movable bed material of D_{50} = 3.1 mm. The effect of the contraction ratio of the stepped spillway was highlighted. Different downstream divergent angle was studied to minimise the scour depth, the results showed that the relative scour depth was reduced by 23% for divergent angle is equal to 170°, different shapes of buffer in stilling basin were also studied to reduce the scour depth where the considered buffer decrease the relative scour depth up to 84%. This study was simulated by Flow 3D program to analyse the scour hole formed using velocity vectors at the bed. The simulated results well agreed with the measured data.

Keywords: buffers, contraction, downstream, Flow 3D, scour, spillway

INTRODUCTION

Stepped spillways ensure that water does not overflow and damage or destroy the dam. The engineering in Greek designed overflow stepped spillway: i.e., an over stepped spillway in Akarnania built around BC 1300 [Chanson 2001]. Many different baffle block shapes have been investigated by Peterka [1978]. Pillai [1989] investigated square conduit, pipe drops, and rectangular stilling basins to determine the sump and stilling basin invert elevations using three explicit equations with (multiple) nonlinear regression techniques. Bormann and Julien [1991], based on two-dimensional jet diffusion and particle stability, studied scour downstream of grade control structures. El-Masry and Sarhan [2000] used a single line of angle baffles for minimising scour downstream heading up the structure. Dargahi [2003] studied experimentally the development of scour profiles. Chanson and Gonzalez [2004] investigated stepped spillways for embankment dams. Azamathulla *et al.* [2006] successfully applied soft computing modelling (artificial neuron network – ANN) to predict scour parameters downstream of ski jump type spillway. Oliveto and Comuniello [2009] provided novel results on the scour processes downstream of positive-step stilling basins considering both equilibrium and time-dependent conditions. Najafzadeh *et al.* [2014] used a group method of data handling (GMDH) to study scour depth downstream of a ski-jump bucket. Koochak and Bajestan [2016] indicated the roughness height of the apron increases, a significant reduction in the scour depth occurs. There are many experimental formulas for local scour due to hydraulic jump in stilling basins, e.g. Novak [1961], Baghdadi [1997], Dargahi [2003], Aytac and Gunal [2008]; Abdelhaleem [2016; 2017]. Awad *et al.* [2018] investigated Minimising Scour of Contraction Stepped Spillways. This paper investigated the contraction of stepped spillways, which increase the scour downstream. Minimising this scour using divergent angle in the downstream spillway or buffers on stilling basins with different shapes were investigated to define the best shape to improve the performance of spillways and minimise the corresponding downstream scour.

MATERIALS AND METHODS

EXPERIMENTAL STUDY

The experimental work was carried out in the hydraulic engineering laboratory, Faculty of Engineering, Zagazig University, Egypt. The flume dimensions were 65 cm depth, 16.2 m length and 66 cm width, as shown in Figure 1. Stepped spillways

© 2021. The Authors. Published by Polish Academy of Sciences (PAN) and Institute of Technology and Life Sciences – National Research Institute (ITP – PIB).
This is an open access article under the CC BY-NC-ND license (https://creativecommons.org/licenses/by-nc-nd/3.0/)

of 4 steps of 32 cm height and 54 cm width, installed on a stilling basin of 120 cm. The discharge measured at the weir was installed downstream of the flume, the used buffers with different dimensions and downstream divergent angles (Fig. 1). In all tests, the used bed material has a median size D_{50} of 3.1 mm [Abdelhaleem *et al.* 2020]. The required time for each test, in which the relationship between d_s and $d_{s\ max}$ was plotted against the time, Figure 2 found that a quasi-equilibrium of maximum scour depth was achieved after 14 400 s, where 90% of the maximum scour depth was achieved. So, each test was carried out over 4 h. The details of experimental conditions are listed in Table 1.

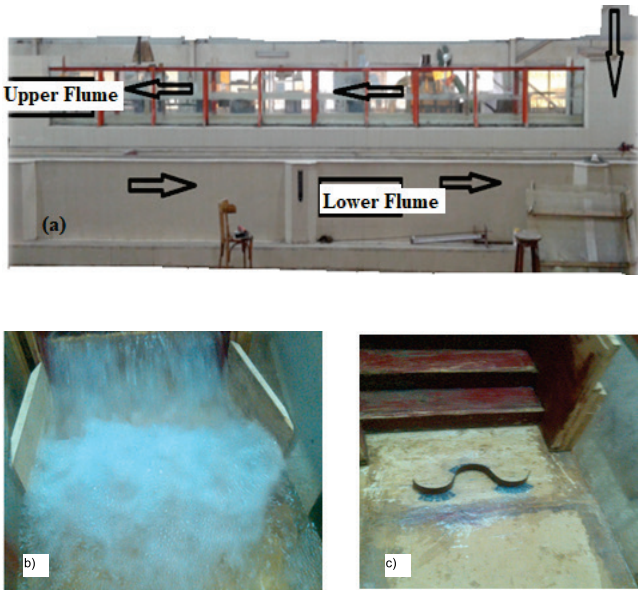

Fig. 1. Laboratory apparatus a) laboratory flume, b) divergent angle, c) shape of buffer in basin models; source: own elaboration

basin models; source: own elaboration

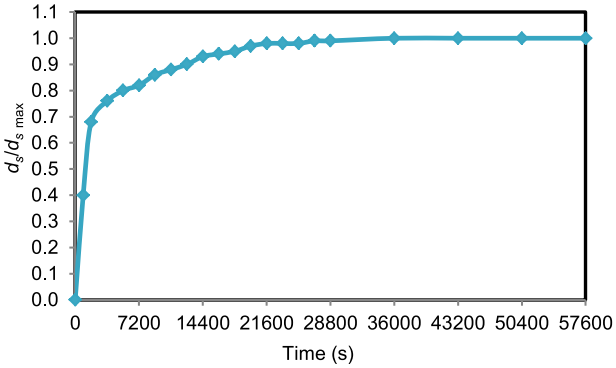

Fig. 2. Relative scour depth versus time for Q = 0.03 m3·s–1; source: own study

SIMULATION USING FLOW 3D MODEL

NUMERICAL STUDY

- Software equations of Flow 3D program

Continuity equation at three dimensional (x, y, z) coordinates is given by:

Table 1. Parameter ranges

Parameter	Unit	Range
Discharge (Q)	$m^3 \cdot s^{-1}$	0.015–0.0352
Slope angle of the spillway (α)	°	30.65
No. of stepped spillway (N)	–	4 steps
Enlargement stilling basin length (L_e)	mm	1065
Length of stilling basin (L_b)	mm	1200
Distance of buffers from spillway (L_2)	mm	255
Height of buffers (h_1)	mm	40
Wide of buffers (b_1)	mm	300
Medium stones size (D_{50})	mm	3.1
Upstream flow depth (H_o)	mm	378–435
Upstream Froude number (F_0)	–	0.018, 0.085

Source: own elaboration.

$$v_f \frac{\partial \rho}{\partial t} + \frac{\partial}{\partial x}(uA_x) + \frac{\partial}{\partial x}(vA_y) + \frac{\partial}{\partial x}(wA_z) = \frac{P_{SOR}}{\rho} \quad (1)$$

where: u, v, w = velocity components in the coordinate directions (x, y and z) directions, A_x, A_y and A_z = cross-sectional areas of flow in the coordinate (x, y and z) directions, ρ = density and P_{SOR} = the source term and v_f is the volume fraction of the fluid.

Three-dimensional momentum equations are given by:

$$\frac{\partial u}{\partial t} + \frac{1}{v_f}\left(uA_x\frac{\partial u}{\partial x} + vA_y\frac{\partial u}{\partial y} + wA_z\frac{\partial u}{\partial z}\right) = \frac{1}{\rho}\frac{\partial P}{\partial x} + G_x + f_x \quad (2)$$

$$\frac{\partial v}{\partial t} + \frac{1}{v_f}\left(uA_x\frac{\partial v}{\partial x} + vA_y\frac{\partial v}{\partial y} + wA_z\frac{\partial v}{\partial z}\right) = \frac{1}{\rho}\frac{\partial P}{\partial x} + G_y + f_y \quad (3)$$

$$\frac{\partial w}{\partial t} + \frac{1}{v_f}\left(uA_x\frac{\partial w}{\partial x} + vA_y\frac{\partial w}{\partial y} + wA_z\frac{\partial w}{\partial z}\right) = z\,\frac{1}{\rho}\frac{\partial P}{\partial x} + G_z + f_z \quad (4)$$

where: P = the pressure of fluid, G_x, G_y and G_z = the body acceleration in the coordinate direction x, y and z, and fx, fy and fz = the viscosity accelerations for coordinate x, y and z.

The control volume of fluid, in the case of a free water surface, f is shown to have a value between 0 and 1. Applying function f to the equation:

$$\frac{\partial F}{\partial t} + \frac{1}{v_f}\left[\frac{\partial}{\partial x}(FA_x u) + \frac{\partial}{\partial y}(FA_y v) + \frac{\partial}{\partial z}(FA_z w)\right] = 0 \quad (5)$$

Steps to solve a problem using Flow 3D software:

- prepare the 3D model of spillway using AutoCAD 3-D software;
- save this file as silt out (STL) file;
- upload the file of STL file in Flow 3-D program, defining the problem in the software and checking the final mesh;
- choose the basic equations which can be solved;
- define the fluid characteristics;

© 2021. The Authors. Published by Polish Academy of Sciences (PAN) and Institute of Technology and Life Sciences – National Research Institute (ITP – PIB).
This is an open access article under the CC BY-NC-ND license (https://creativecommons.org/licenses/by-nc-nd/3.0/)

- define the boundary conditions, where it is notable that this software has a wide range of boundary conditions (Fig. 3);
- initialise the flow field (Fig. 4);
- adjust the output;
- select the calculation method and solution formula after adjusting the control parameters;
- start the calculation and get results (Fig. 5).

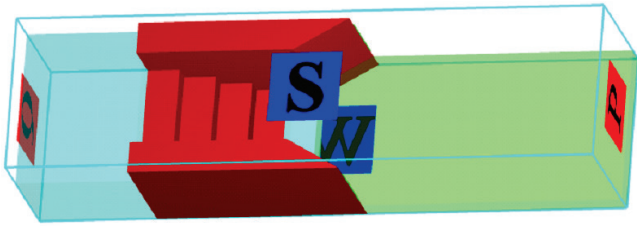

Fig. 3. The boundary of the contracted spillway with divergent angle was: inlet = discharge (*Q*), outlet = pressure (*p*), two sides and bed = wall (w) and up water = symmetry (s); source: own elaboration

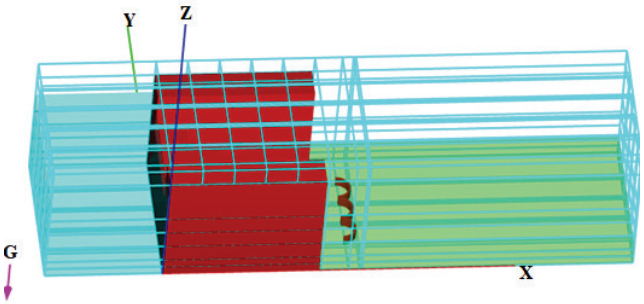

Fig. 4. Grid and axis of buffer for contracted stepped spillway; source: own elaboration

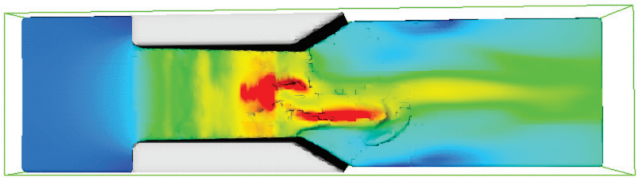

Fig. 5. Water flow through contracted stepped spillway with divergent angle θ = 170° by Flow 3D program; source: own elaboration

DIMENSIONAL ANALYSIS

The maximum scour depth downstream stepped spillway $d_{s\ \max}$ can be expressed as a function of the following independent variables as shown in Equation (6) (Fig. 6).

$$d_{smax} = f(y_1, y_c, y_2, y_t, B, H, b, h_s, b_s, \theta, h_1, L_1, L_2, L_e, b_1, v_o, v_1, v_2, v_t, H_o, C, \rho, D_{50}, \mu, \alpha, g) \quad (6)$$

But some of these variables were constant as *B, H,* ρ, D_{50}, μ, α, *g* so Equation (6) can be written as:

$$d_{smax} = f(C, \theta, v_o, \rho, H_o, g) \quad (7)$$

By applying the Buckingham theorem and choosing ρ, H_o, and *g*, as repeated variables, Equation 7 can be written in dimensionless form as follows:

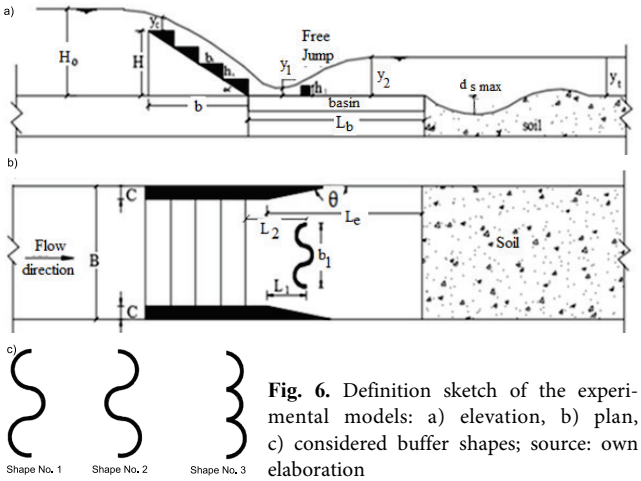

Fig. 6. Definition sketch of the experimental models: a) elevation, b) plan, c) considered buffer shapes; source: own elaboration

$$\frac{d_{s\ \max}}{H_o} = f\frac{d_{s\ \max}}{H_o} = f\left(\frac{C_o}{B}, \theta, \mathrm{F}_0\right) \quad (8)$$

where $d_{s\ \max}$ = maximum scour depth in flume, y_1 = the primary water depth of hydraulic jump, y_c = critical water depth $\left(\sqrt[3]{\frac{q^2}{g}}\right)$, q = specific discharge $\left(\frac{Q}{B}\right)$, Q = the discharge rate in the channel, y_2 = the sequent water depth of hydraulic jump, y_t = the downstream water depth in the channel, B = channel width, H = the spillway height, b = the spillway length, h_s = the step height, b_s = the step width, θ= slope angle of side wall in spillway, h_1 = the buffer height, L_1 = the distance between the buffer place and the start point of enlargement, L_2 = the distance between spillway and the buffer place, L_e = the length between the start point of enlargement and the end of stilling basin, b_1 = the buffer width, v_o = the upstream velocity of the spillway, v_1 = the velocity at the beginning of the free hydraulic jump, v_2 = the velocity at the end of the free hydraulic jump, v_t = the downstream velocity of the channel, H_o = water depth in upstream of spillway, C = side wall width, ρ = the density of water, D_{50} = medium stones size, μ = the dynamic viscosity of water, α = the spillway slope angle, g = the acceleration due to gravity, C_o = step width of spillway (B – 2C), F_0 = Froude number of flume in upstream of spillway.

RESULTS AND DISCUSSION

EFFECT OF CONTRACTION RATIO

The effect of contraction ratio on local scour depth was experimentally studied, whereas the relative contraction ratio (C_o/B) was changed four times to be 0.9, 0.8, 0.7 and 0.6. The relationship between the maximum relative scour depth ($d_{s\ \max}/H_o$) and Froude number (F_0) for different relative contraction ratios are shown in Figure 7. This figure illustrates how the maximum relative scour depth increases as the Froude number increases. Increasing the contraction ratio leads to an increase of velocity and therefore increases the scour. Figure 8 shows the relationship between $d_{s\ \max}/H_o$ for different relative contraction ratio (C_o/B) at upstream F_0 = 0.082, which explains that the lowest relative value of scour depth occurs at stepped spillway without contraction and the case of C_o/B = 0.6 gives the highest one. Figures 9 and 10 illustrate the scour contour map for bed morphology from experimental readings and velocity vectors from Flow 3D program at F_0 = 0.047 for relative contraction ratio

© 2021. The Authors. Published by Polish Academy of Sciences (PAN) and Institute of Technology and Life Sciences – National Research Institute (ITP – PIB).
This is an open access article under the CC BY-NC-ND license (https://creativecommons.org/licenses/by-nc-nd/3.0/)

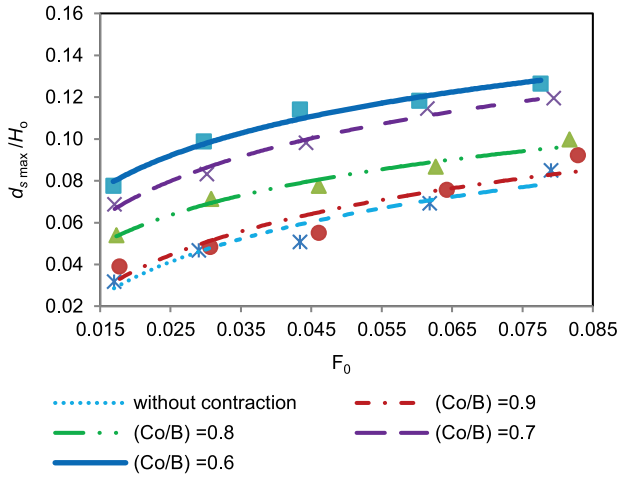

Fig. 7. Relationship between maximum relative scour depth ($d_{s\ max}/H_o$) and Froude number F_0 at different relative contracted ratios (C_o/B); source: own study

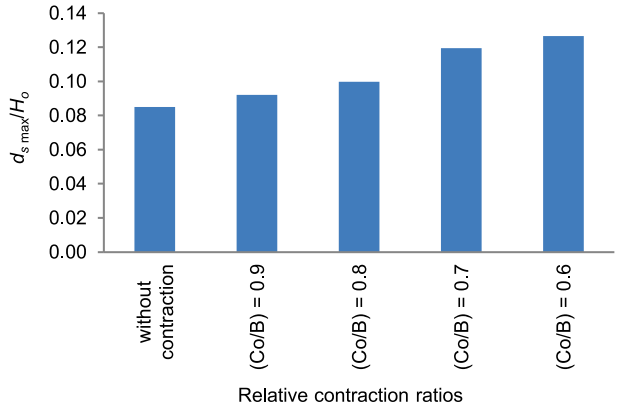

Fig. 8. Relationship between maximum relative scour depth ($d_{s\ max}/H_o$) for different relative contracted ratios (C_o/B) at Froude number F_0 = 0.082; source: own study

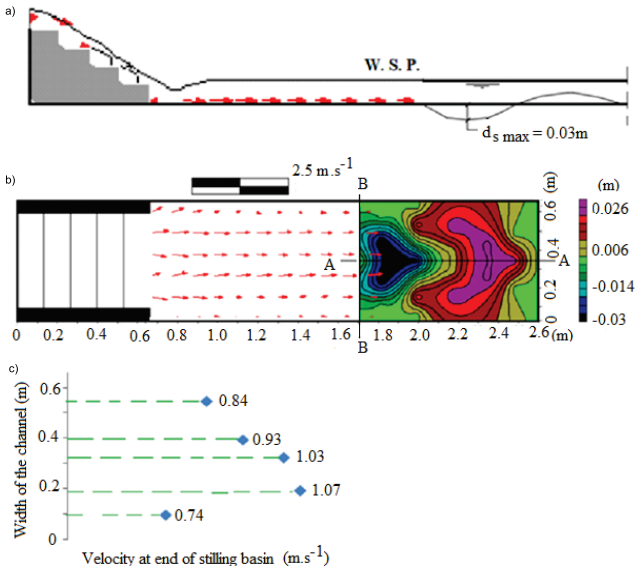

Fig. 9. Scour contour map for bed morphology and velocity vectors for relative contracted ratios C_o/B = 0.9 at Froude number F_0 = 0.047: a) section elevation at A–A, b) section plan, c) section velocity at B–B; source: own study

C_o/B = 0.9 and C_o/B = 0.6 respectively. These figures show that the velocities at the axis of the channel were higher than the velocities in the two sides, so the scour hole formed in the middle. Also, by comparing Section (B–B) in Figures 9 and 10, we find that the values of velocities in case C_o/B = 0.6 are higher than its values for case C_o/B = 0.9. Section elevation (A–A) explains the water surface profile (W.S.P.) using the Flow 3D program and maximum scour hole using experimental readings.

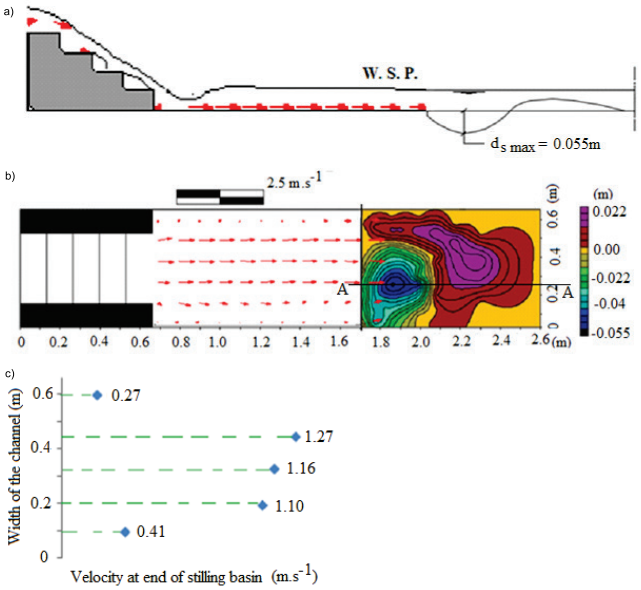

Fig. 10. Scour contour map for bed morphology and velocity vectors for relative contracted ratios C_o/B = 0.6 at Froude number F_0 = 0.047: a) section elevation at A–A, b) section plan, c) section velocity at B–B; source: own study

EFFECT OF DOWNSTREAM DIVERGENT ANGLE

The effect of downstream divergent angle on local scour depth was studied experimentally where it changed four times to 90°, 135°, 150° and 170° as shown in Figure 11, which explains the relationship between the maximum relative scour depth ($d_{s\ max}/H_o$) and Froude number (F_0). This figure shows that the maximum relative scour depth increases as F_0 increases. For lower values of upstream F_0, the relative scour depth values close to each other, while for higher values of upstream F_0 the relative scour depth values separated to each other because of increasing the discharge rate. Also, increasing downstream divergent angle (θ) leads to increasing the cross-sectional area and hence decreasing the velocity, so the scour decreases. The downstream divergent angles (θ) are equal to 135°, 150° and 170° reduce relative scour depth by 5, 12 and 23%, respectively as shown in Figure 12. Scour contour map for bed morphology and velocity vectors at upstream Froude number (F_0) = 0.08 for the downstream divergent angle (θ) is equal to 90°, 135° and 170° are shown in Figures 13 and 14, respectively. This is because the velocities in the channel axis are higher than the velocities in the sides. Therefore the maximum scour hole was formed in the middle, also increasing downstream divergent angle (θ), leading to a decrease in the velocities as shown in Section (B–B) for the

© 2021. The Authors. Published by Polish Academy of Sciences (PAN) and Institute of Technology and Life Sciences – National Research Institute (ITP – PIB).
This is an open access article under the CC BY-NC-ND license (https://creativecommons.org/licenses/by-nc-nd/3.0/)

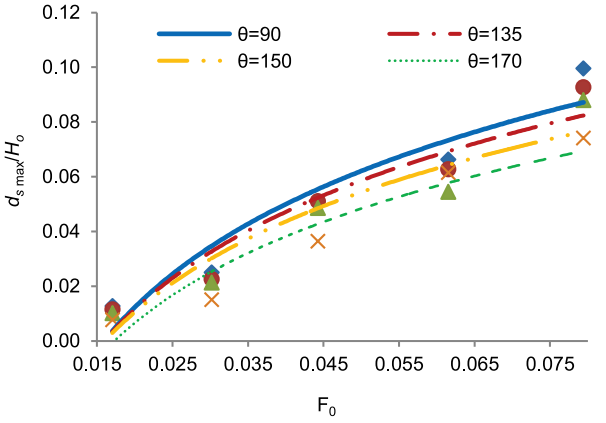

Fig. 11. Relationship between maximum relative scour depth ($d_{s\ max}/H_o$) and Froude number (F_0) for different divergent angles (θ); source: own study

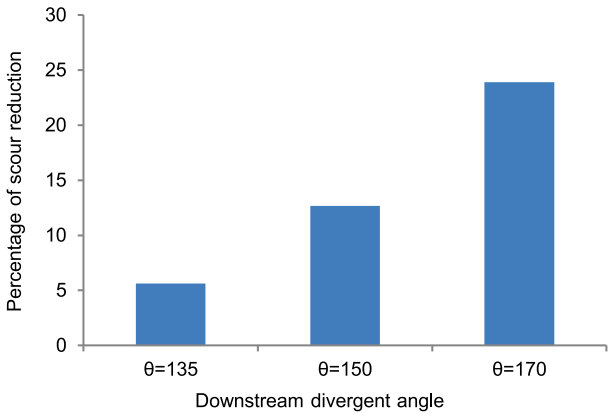

Fig. 12. Relationship between percentage of scour reduction and different downstream divergent angle (θ); source: own study

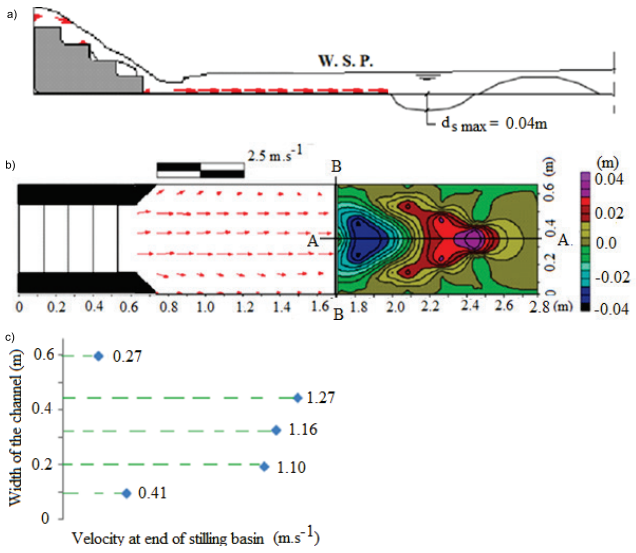

Fig. 13. Scour contour map for bed morphology and velocity vectors for divergent angle θ = 135° at Froude number F_0 = 0.08: a) section elevation at A–A, b) section plan, c) section velocity at B–B; source: own study

previous figures. Section (A–A) shows the water surface profile resulting from Flow 3D program. Also, it illustrates the maximum scour depth from experimental reading.

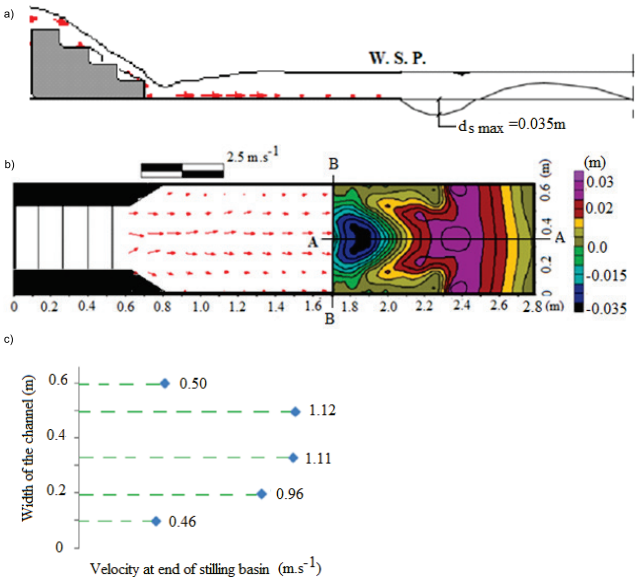

Fig. 14. Scour contour map for bed morphology and velocity vectors for divergent angle θ = 170° at Froude number F_0 = 0.08: a) section elevation at A–A, b) section plan, c) section velocity at B–B; source: own study

EFFECT OF DIFFERENT SHAPES OF BUFFERS

The buffer was placed in the stilling basin so that it consists of three half-cylinders connected to each other with $h_1 = 0.5h_s$, $b_1 = 0.45B$, and $L_2 = 0.21L_b$, as shown in Figure 15. The effect of different shapes of buffers on the scour was investigated experimentally. The shapes of buffers are changed three times, as shown in Figure 16. Figure 17 explains the relationship between the maximum relative scour depth ($d_{s\ max}/H_o$) and Froude number (F_0) for different shapes of buffers. This figure shows that the maximum relative scour depth increases as F_0 increases. Also, it can be concluded that shape No. 3 gives the least values of scour depth. The scour was reduced by 52, 79 and 84% for shapes No. 1, 2 and 3. Figures 17 and 18 show the scour contour map for bed morphology and velocity vectors for shapes No. (1 and 3 at F_0 = 0.08, it could be observed from section (B–B) in these figures that the least utmost velocity occurs in case of shape No. (3), so it gives the minimum scour depth.

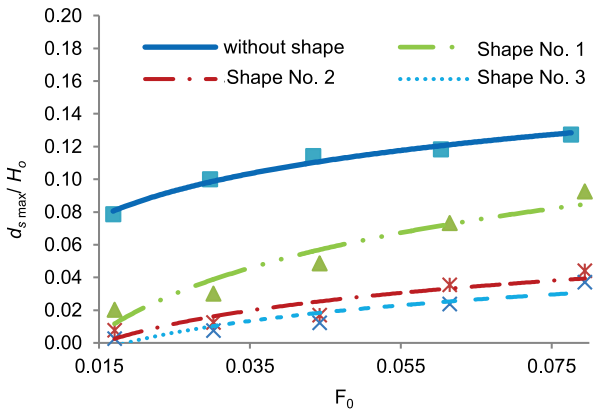

Fig. 15. Relationship between the maximum relative scour depth ($d_{s\ max}/H_o$) and Froude number F_0 for different shapes of buffer; source: own study

© 2021. The Authors. Published by Polish Academy of Sciences (PAN) and Institute of Technology and Life Sciences – National Research Institute (ITP – PIB).
This is an open access article under the CC BY-NC-ND license (https://creativecommons.org/licenses/by-nc-nd/3.0/)

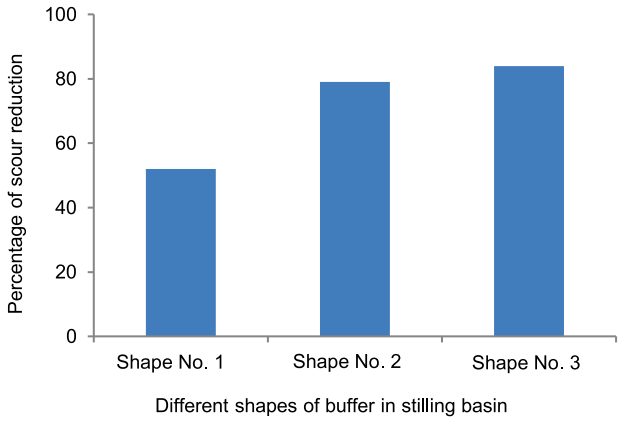

Fig. 16. Relationship between percentage of scour reduction and different shapes of buffer; source: own study

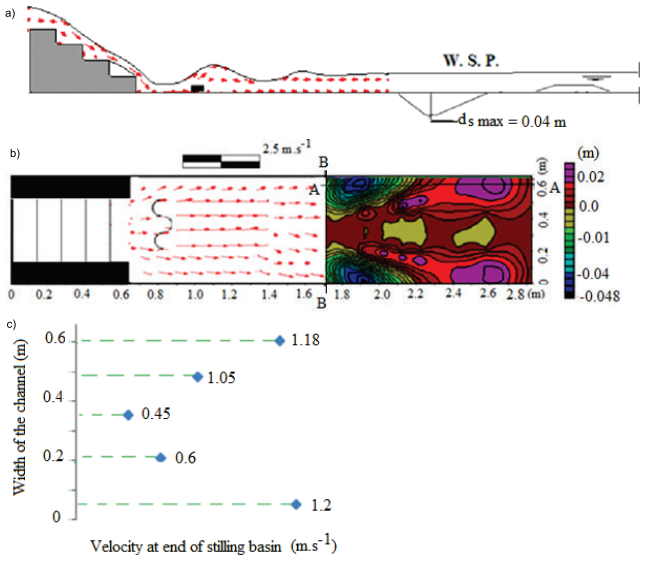

Fig. 17. Scour contour map for bed morphology and velocity vectors for shape No. 1 and Froude number F_0 = 0.08: a) section elevation at A–A, b) section plan, c) section velocity at B–B; source: own study

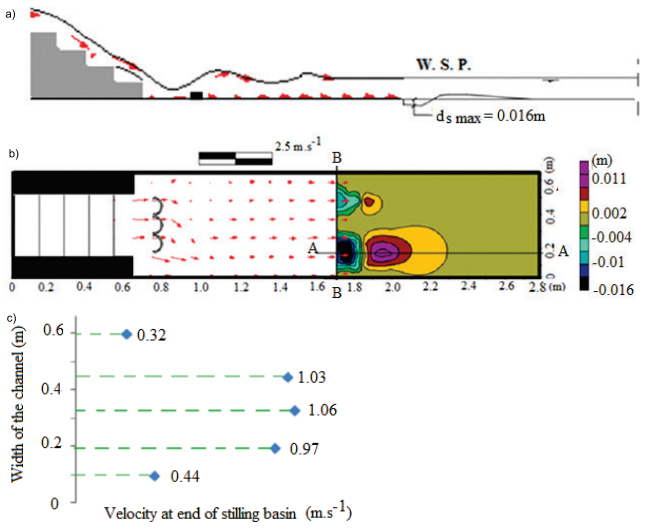

Fig. 18. Scour contour map for bed morphology and velocity vectors for shape No. 3 and Froude number F_0 = 0.08: a) section elevation at A–A, b) section plan, c) section velocity at B–B; source: own study

CALIBRATION OF EXPERIMENTAL MEASUREMENTS

Predicting the maximum scour depth ($d_{s\ max}$) for the different cases under investigation is important because the ds max is an important design factor. Figure 19 shows a comparison between the experimental results for the present study in case of divergent angle equal to 170° and shape of buffers No. 3 and studies given by Dargahi [2003], Elnekhily [2016] and Abdelhaleem [2017]. It is observed that the empirical of Dargahi [2003] give higher values of $d_{s\ max}/H_o$ than those calculated by other equations; this may be due to the variation of particle size of material (d_{90}). On the other hand, other equations give very close values of the scour depth obtained from the present study. Among these equations, Abdelhaleem [2013] and Elnikhely [2016] equations gave a good estimate of the measured scour depth.

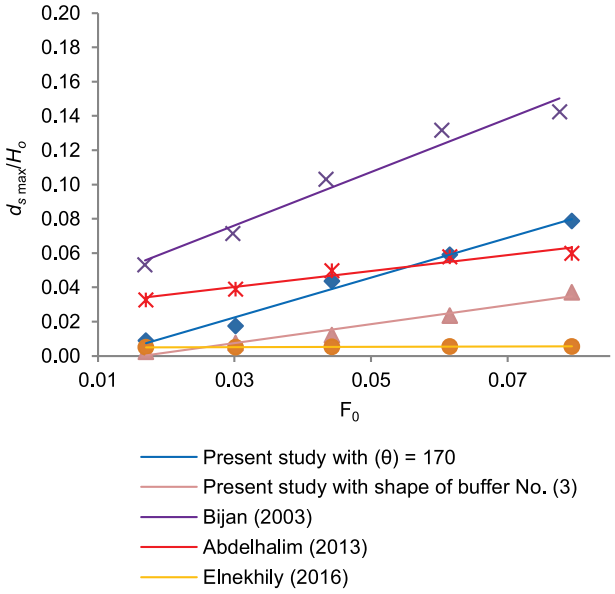

Fig. 19. Comparison of measured and computed maximum relative scour depths ($d_{s\ max}/H_o$) with maximum relative scour depth given by other studies as a function of Froude number F_0; source: own study

STATISTICAL ANALYSIS

The phenomena of this model analyses by using regression analysis, the correlation coefficients and standard errors of Equation (9), is (89%, 0.01) respectively, predicted equations for different simulated models were created as follows:

$$\frac{d_{s\ max}}{H_o} = 0.23 + 0.89F_0 - 0.14\frac{C_o}{B} - 0.001\theta \qquad (9)$$

Where limitation of this equation: F_0 = 0.018 to 0.085, C_o/B = 0.6 to 0.9 and θ = 90–170°

The relation between measured and predicted data of the maximum relative scour is shown in Figure 20. It could be observed from this figure that the predicted equations express well the measured data.

© 2021. The Authors. Published by Polish Academy of Sciences (PAN) and Institute of Technology and Life Sciences – National Research Institute (ITP – PIB).
This is an open access article under the CC BY-NC-ND license (https://creativecommons.org/licenses/by-nc-nd/3.0/)

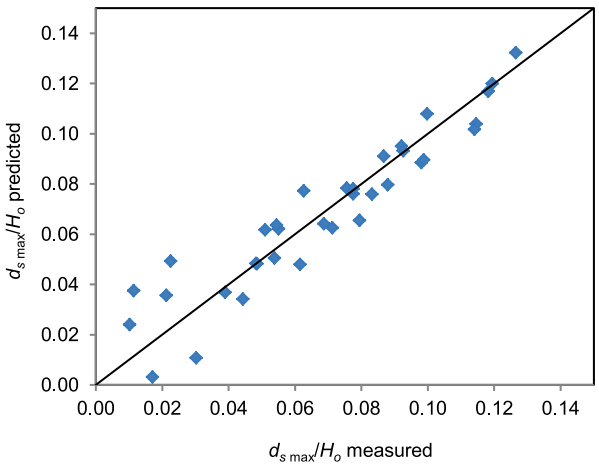

Fig. 20. Comparison between predicted and measured data for maximum relative scour depth ($d_{s\ max}/H_o$); source: own study

CONCLUSIONS

1. The maximum relative depth of scour increases with increasing value the upstream Froude number (F_0).
2. Scour depth increases with increasing value contraction ratio.
3. Increasing downstream divergent angle (θ) leads to decreasing scour hole.
4. The downstream divergent angle (θ) reduces relative scour depth by 5, 12 and 23% for downstream divergent angle (θ) equal to 135, 150 and 170°
5. The best shape of buffers at the stilling basin is shape 3, which reduced the scour by 84% compared with the case of without buffers.
6. The scour reduced by 52, 79 and 84% for shapes No. 1, 2 and 3, respectively.
7. Flow 3D program can be used for simulating the scour phenomena.
8. The proposed equation for predicting relative scour depth was well agreeable with the measured data.

REFERENCES

Abdelhaleem F.S. 2013. Effect of semi-circular baffle blocks on local scour downstream clear-overfall weirs. Ain Shams Engineering Journal. Vol. 4 p. 675–684. DOI 10.1016/j.asej.2013.03.003.

Abdelhaleem F.S. 2016. Discharge estimation for submerged parallel radial gates. Flow Measurement and Instrumentation. Vol. 52 p. 240–245. DOI 10.1016/j.flowmeasinst.2016.11.001.

Abdelhaleem F.S. 2017. Hydraulics of submerged radial gates with a sill. ISH Journal of Hydraulic Engineering. Vol. 23(2) p. 177–186. DOI 10.1080/09715010.2016.1273798.

Abdelhaleem F.S., Amin A.M., Basiouny M.E., Ibraheem H.F. 2020. Adaption of a formula for simulating bedload transport in the Nile River, Egypt. Journal of Soils and Sediments. Vol. 20(3) p. 1742–1753. DOI 10.1007/s11368-019-02528-8.

Awad A.S., Nasr-Allah T.H., Mohamed Y.A., Abdel-Aal G.M. 2018. Minimizing scour of contraction stepped spillways. Journal of Engineering Research and Reports. Vol. 1(1), 41543 p. 1–11. DOI 10.9734/jerr/2018/v1i19779.

Aytac S., Gunal M. 2008. Prediction of scour downstream of grad control structures using neural networks. Journal of Hydraulic Engineering. Vol. 10(11) p. 1656–1660. DOI 10.1061/(ASCE)0733-9429(2008)134:11(1656).

Azamathulla H.M., Deo M.C., Deolalikar P.B. 2006. Estimation of scour below spillways using neural networks. Journal Hydraulic Research, International Association Hydraulic Research. Vol. 44 (1) p. 61–69. DOI 10.1080/00221686.2006.9521661.

Baghdadi K.H. 1997. Local scour downstream drop structure. Alexandria Engineering Journal. Vol. 36. No. 2.

Bormann N.E., Julien P.Y. 1991. Scour downstream of grade-control structures. Journal of Hydraulic Engineering. Vol. 117(5) p. 579–594. DOI 10.1061/(ASCE)0733-9429(1991)117:5(579).

Chanson H. 2001. The hydraulics of stepped chutes and spillways. Lisse, The Netherlands. Balkema. ISBN 90-5809-352-2 pp. 418.

Chanson H., Gonzalez C.A. 2004. Stepped spillways for embankment dams. Review, progress and development in overflow hydraulic. In: Hydraulics of dams and river structures. Eds. F. Yazdandoost, J. Attari. Proceedings of the International Conference. Tehran, Iran, 26–28 April 2004. London. Taylor & Francis Group p. 287–294.

Dargahi B. 2003. Scour development downstream of a spillway. Journal of Hydraulic Research. Vol. 41(4) p. 417–426. DOI 10.1080/00221680309499986.

El-Masry A.A, Sarhan T.E. 2000. Minimization of scour downstream heading-up structure using a single line of angle baffles. Engineering Research Journal. Vol. 69 p. 192–207.

Elnikhely E.A. 2016. Minimizing scour downstream of spillways using curved vertical sill. International Water Technology Journal. Vol. 6. No. 3.

Koochak P., Bajestan M.S. 2016. The effect of relative surface roughness on scour dimensions at the edge of horizontal apron. International Journal of Sediment Research. Vol. 31(2) p. 159–163. DOI 10.1016/j.ijsrc.2013.02.001.

Najafzadeh M., Barani G.A., Kermani M.R. 2014. Group method of data handling to predict scour at downstream of a ski-jump bucket spillway. Earth Science Informatics. Vol. 7(4) p. 231–248. DOI 10.1007/s12145-013-0140-4.

Novak P.J. 1961. Influence of bed load passage on scour and turbulence downstream of stilling basin. Congress, IAHR, Dubrovnik, Croatia.

Oliveto G., Comuniello V. 2009. Local scour downstream of positive-step stilling basins. Journal of Hydraulic Engineering. Vol. 135 (10) p. 846–851. DOI 10.1061/(ASCE)HY.1943-7900.0000078.

Peterka A.J. 1978. Hydraulic design of stilling basin and energy dissipaters [online]. A Water Resources Technical Publication. Engineering Monograph. No. 95. Denver. U.S. Dept. of the Interior. Bureau of Reclamation. [Access 12.12.2020]. Available at: https://www.usbr.gov/tsc/techreferences/hydraulics_lab/pubs/EM/EM25.pdf

Pillai N.N. 1989. Hydraulic jump type stilling basin for low Froude numbers. Journal of Hydraulic Engineering. Vol. 115(7) p. 989–994. DOI 10.1061/(ASCE)0733-9429(1989)115:7(989).

© 2021. The Authors. Published by Polish Academy of Sciences (PAN) and Institute of Technology and Life Sciences – National Research Institute (ITP – PIB).
This is an open access article under the CC BY-NC-ND license (https://creativecommons.org/licenses/by-nc-nd/3.0/)